SUPPLEMENTARY INFORMATION

Rapid elongation drives the exceptionally fast aggregation of medin, the most common localized human amyloid

Vaidehi Roy Chowdhury[1], Robert I. Horne[1], Mariana P. Cali[1], Zenon Toprakcioglu[1], Sara Linse[2] and Michele Vendruscolo[1,*]

[1]*Centre for Misfolding Diseases, Yusuf Hamied Department of Chemistry, University of Cambridge, Lensfield Road, Cambridge CB2 1EW, United Kingdom*
[2]*Biochemistry and Structural Biology, Department of Chemistry, Lund University, SE-221 00 Lund, Sweden*

Fitting of the aggregation data using kinetic models

The integrated rate law equation used for fitting data of aggregation reactions with an initial monomer mass concentration m_0 and aggregate mass concentration M at any time to a secondary nucleation dominated model is [1]:

$$\frac{M}{M_\infty} = 1 - (1 - \frac{M_0}{M_\infty})e^{-k_\infty t}.(\frac{B_- + C_+e^{\kappa t}}{B_+ + C_+e^{\kappa t}} \cdot \frac{B_+ + C_+}{B_- + C_+})^{\frac{k_\infty}{\kappa k_\infty}} \quad (1)$$

where the parameters are defined as

$$\kappa = \sqrt{2m_0k_+m_0^{n_2}k_2} \quad (2)$$

$$\lambda = \sqrt{2k_+k_nm_0^{n_c}} \quad (3)$$

$$C_\pm = \frac{k_+P_0}{\kappa} \pm \frac{k_+M_0}{2m_0k_+} \pm \frac{\lambda^2}{2\kappa^2} \quad (4)$$

$$k_\infty = \sqrt{(2k_+P_0)^2 + \frac{4k_+k_nm_0^{n_c}}{n_c} + \frac{4k_+k_2m_{tot}m_0^{n_2}}{n_2} + \frac{4k_+k_2m_0^{n_2+1}}{n_2+1}} \quad (5)$$

$$\bar{k}_\infty = \sqrt{k_\infty^2 - 2C_+C_-\kappa^2} \quad (6)$$

$$B_\pm = \frac{k_\infty \pm \bar{k}_\infty}{2\kappa} \quad (7)$$

and where

m_0 is the monomer mass concentration at time $t = 0$,

M_0 is the aggregate mass concentration at time $t = 0$ (which is equal to 0 under unseeded conditions),

P_0 is the aggregate number concentration at time $t = 0$ (which is equal to 0 under unseeded conditions),

M_∞, the mass at long times, is just the total protein mass concentration, m_{tot},

k_+ is the elongation rate constant,

k_n is the primary nucleation rate constant,

k_2 is the secondary nucleation rate constant,

k_{off} is the dissociation rate constant,

n_c is the primary nucleation order,

n_2 is the secondary nucleation order.

The off-rate is considered negligible, i.e., $k_{\text{off}} \ll k_+ m_0$. In the unseeded case this depends only on the combined rate constants $k_+ k_n$ and $k_+ k_2$, not k_+, k_2 and k_n individually. The approximate scaling exponent is:

$$\gamma \approx -\frac{n_2 + 1}{2} \tag{8}$$

The integrated rate law equation used for fitting data of an aggregation reaction to a fragmentation dominated model is [1]:

$$M = M_\infty + Exp\left[-\frac{k_+(4c\kappa\, cosh(\kappa t) + 4P_0\kappa^2\, sinh(\kappa t))}{2\kappa^3}\right]\left((M_0 - M_\infty)e^{\frac{2k_+c}{k^2}}\right) \tag{9}$$

where the parameters are defined as

$$\begin{aligned} c &= k_n m_0^{n_c} + k_- M_0 \\ \kappa &= \sqrt{2\left(k_+ m_0 - k_{off}\right)k_-} \\ M_\infty &= m_{tot} - {k_{off}}/{k_+} \end{aligned} \tag{10}$$

and where

k_- is the fragmentation rate constant.

In the unseeded case, for negligible k_{off}, this depends only on the combined rate constants $k_+ k_n$ and $k_+ k_-$, not k_+, k_n and k_- individually. The approximate scaling exponent is:

$$\gamma = -\frac{1}{2} \tag{11}$$

$$\ln \alpha_{A\beta_{42}} = -15.9$$
$$\gamma_{A\beta_{42}} = -1.2$$

$\therefore$ from (15),

$$\ln m_{A\beta_{42}} = \frac{5 \ln m_{medin} - 85}{12}$$
$$\Longrightarrow m_{A\beta_{42}} = \frac{(m_{medin})^{5/12}}{1192} \tag{16}$$

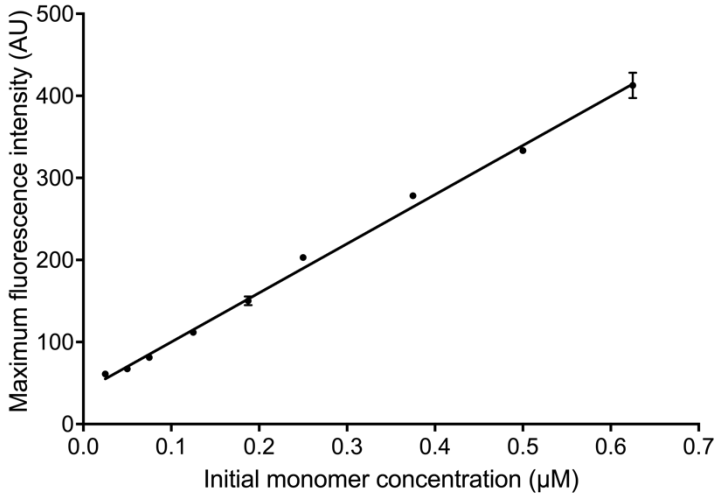

Figure S1. ThT fluorescence response against the initial monomer concentration. The maximum fluorescence intensity at the plateau of the sigmoidal curves depends linearly on the initial monomer equivalents required to form fibrils ($\boldsymbol{R^2 = 0.99}$). Data are presented as mean ± SEM.

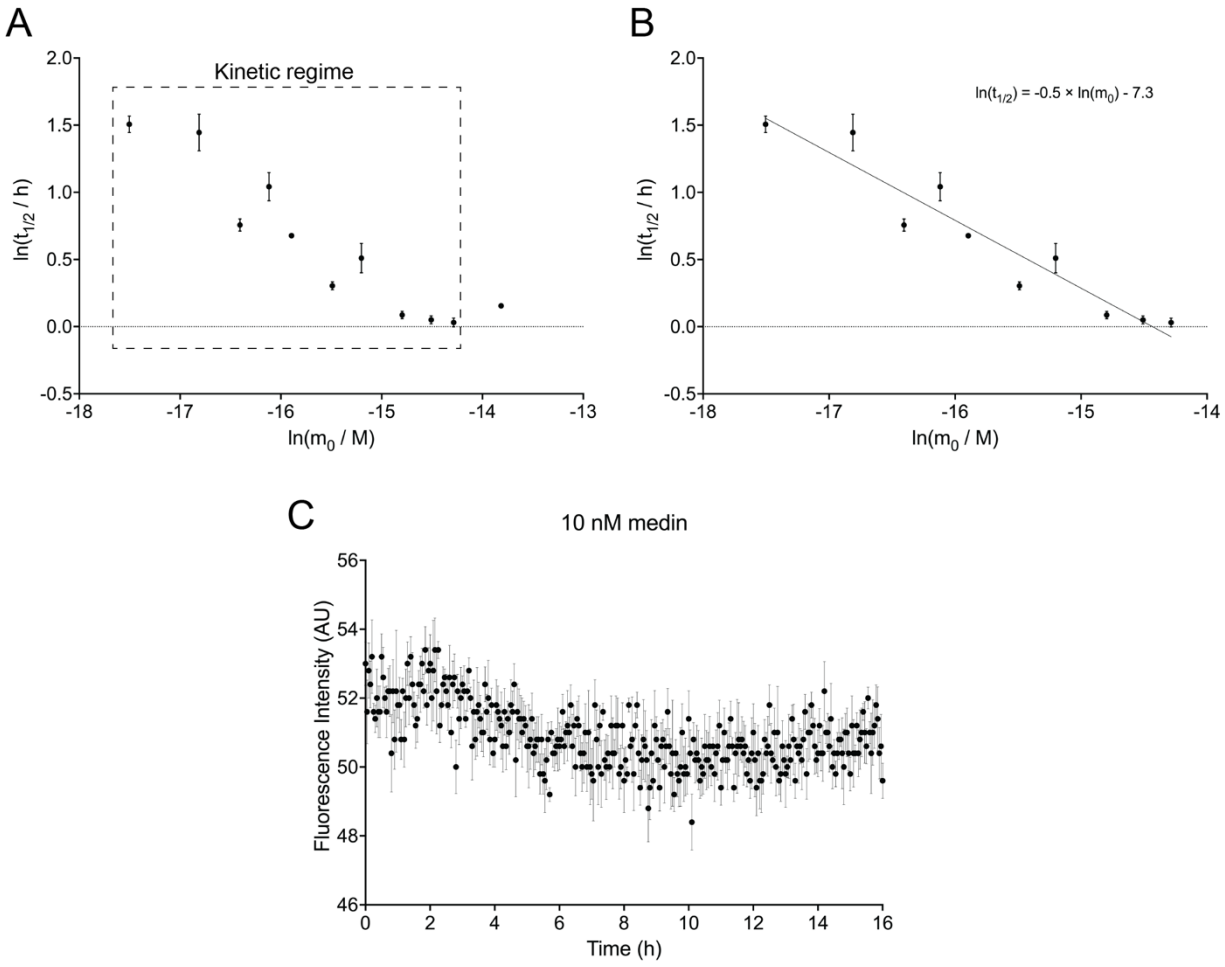

Figure S2. Choice of the concentration for the determination of the aggregation mechanism. (A) Medin aggregation was monitored at a range of monomer concentrations spanning the physiological range (0-14 μM). The data points shown here correspond to 25-1000 nM. **(B)** A negative scaling of the logarithm of $t_{1/2}$ to the logarithm of m_0 was observed only until 625 nM, which defined the upper boundary of the kinetic regime that we investigated in this work. **(C)** Below 25 nM, e.g. at 10 nM, no aggregation was observed within the reaction timescale. Thus, we considered 25 nM as an estimate of the critical concentration. Data are presented as mean ± SEM.

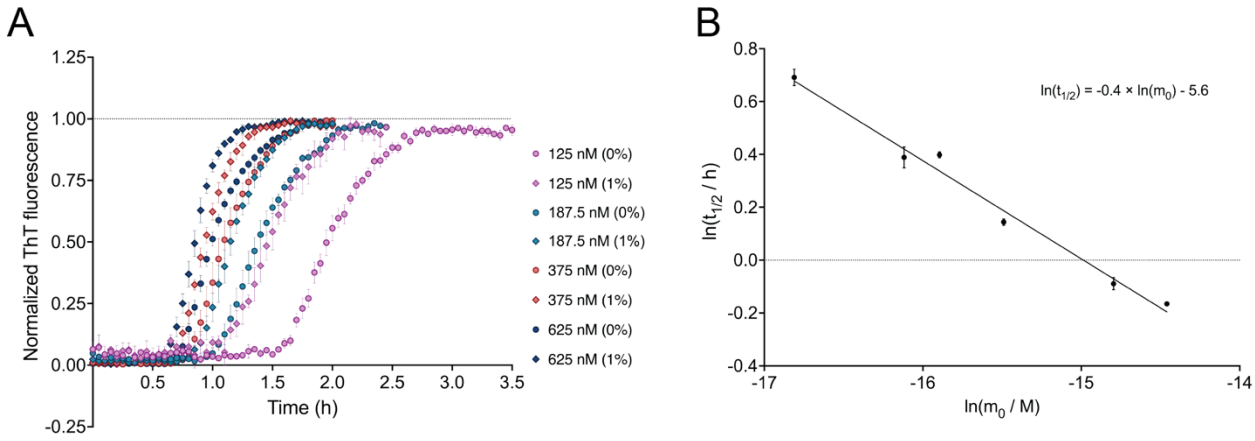

Figure S3. Comparison of half-times of unseeded and low-seeded aggregation reactions. (A) Both the t_{lag} and $t_{1/2}$ are reduced when a small quantity of pre-formed fibrils is added as seeds to the aggregation reaction, thus confirming the secondary nature of medin aggregate proliferation under physiological conditions *in vitro*. Seed:monomer ratios are given in parentheses in the legend. (B) Addition of 1% seeds does not significantly alter the mechanism of aggregation nor the weak monomer dependence of nucleation events (R^2 = 0.96). Data are presented as mean ± SEM.

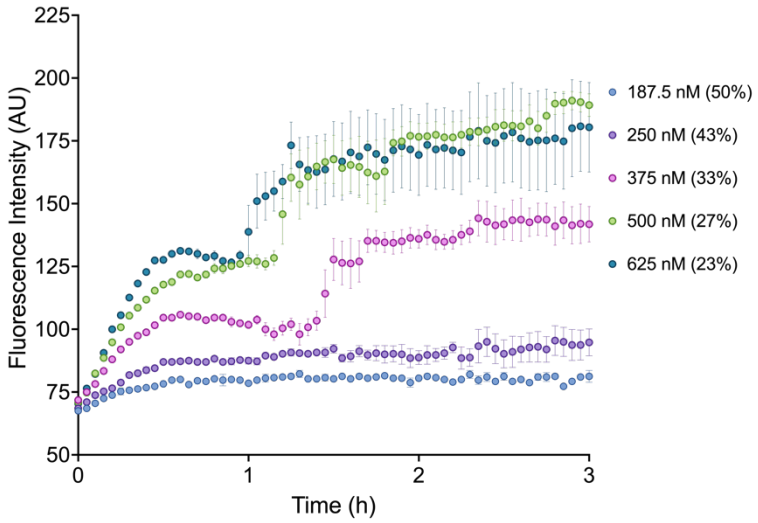

Figure S4. Biphasic aggregation time-course in high-seeded conditions. Within the total protein concentration regime of 562.5-812.5 nM, there is a typical biphasic aggregation profile, where the reaction stabilizes temporarily before quickly (within 9 min) spiking to a second, higher plateau. The data analysis was done considering the first plateau only. Data are presented as mean ± SEM; AU = arbitrary unit.

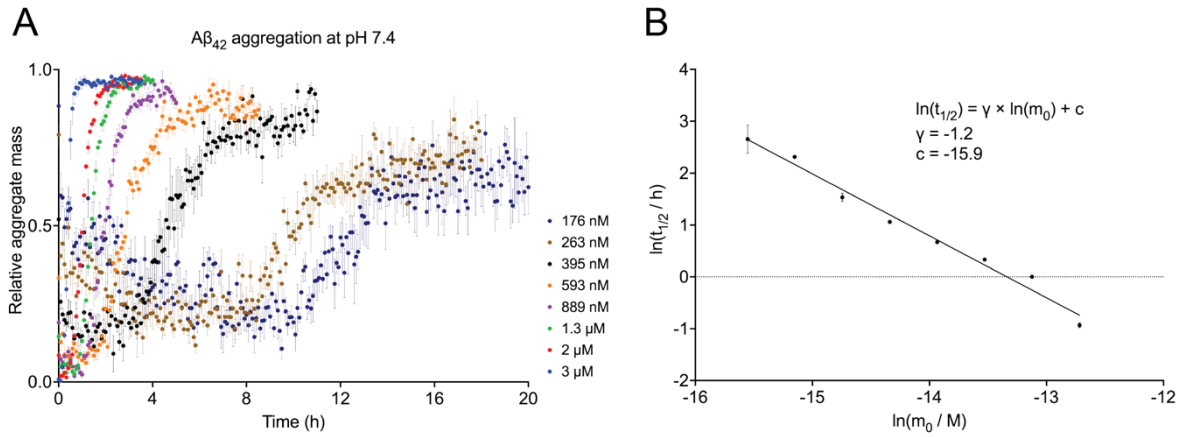

Figure S5. Scaling of half-times with initial monomer concentration of Aβ42. (A) Recombinant human Aβ42 was incubated at 37 °C quiescently in 20 mM NaPi 0.2 mM EDTA pH 7.4 in 96-well half-area non-binding plates (Corning 3881), with 100 µL per well (n = 5). An aluminium film coating minimized evaporation. Aggregation was monitored using 20 µM ThT. No aggregation was observed at concentrations below 117 nM within 26.5 hours. **(B)** The half-time ($t_{1/2}$) of each reaction depends inversely on the initial monomer concentrations (m_0) with a scaling exponent γ = -1.2, which is characteristic of secondary nucleation (R^2 = 0.96). Data are presented as mean ± SEM.

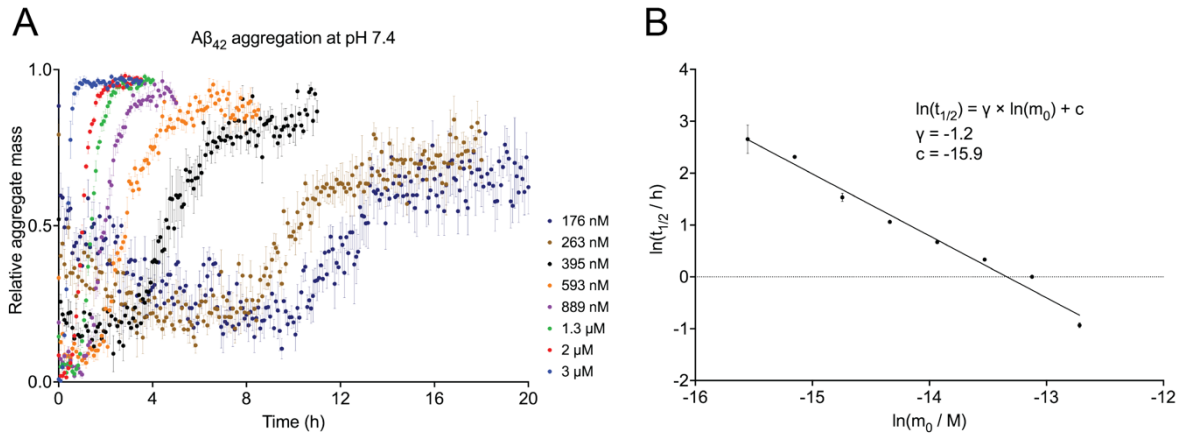
A
Aβ42 aggregation at pH 7.4
Relative aggregate mass
Time (h)
176 nM
263 nM
395 nM
593 nM
889 nM
1.3 µM
2 µM
3 µM
B
ln(t1/2) = γ × ln(m0) + c
γ = -1.2
c = -15.9
ln(t1/2 / h)
ln(m0 / M)

Table S1. Sequence analysis of recombinant medin by tryptic digestion LC-MS/MS. All fragments bigger than 500 Da were detected (unlike previous reports).

Amino acid sequence of tryptic digest product	**Mean calculated mass (Da)**	**Mean observed mass (Da)**
QGNFNAWVAGSYGNDQWLQVDLGSSK	2840.312	2840.3181
EVTGIITQGAR	1143.625	1143.6246
NFGSVQFVA	967.9681	967.9684

Table S2. Values of fitted kinetic parameters obtained individually from aggregation assays at high-seeded, low-seeded and unseeded conditions.

Parameter	Symbol	Unit	Model chosen	Mean squared error (MSE)	Fit results
Elongation rate constant	k_+	M^{-1} s^{-1}	Fragmentation dominated	0.00482	5.4E+07
			Secondary nucleation dominated	0.00484	5.3E+07
Secondary pathway rate constant	k_-	s^{-1}	Fragmentation dominated	0.02696	4.3E-08
	k_2	s^{-1}	Secondary nucleation dominated	0.02688	4.4E-08
Secondary nucleation Order	n_2	Unitless	Secondary nucleation dominated	0.02688	~0
Combined rate constant	k_+k_n	$M^{-1}s^{-2}$	Fragmentation dominated, no seed	0.031	3.3E-01
			Secondary nucleation dominated, no seed	0.039	2.3E-02
Primary nucleation order	n_c	Unitless	Fragmentation dominated, no seed	0.031	~1
			Secondary nucleation dominated, no seed	0.039	~1

Table S3. Values of fitted kinetic parameters from global data analysis. The MSEs for both the fragmentation dominated and for secondary nucleation dominated model are 0.02.

Parameter	**Symbol**	**Unit**	**Model chosen**	**Fit results**
Elongation rate constant	k_+	M^{-1} s^{-1}	Fragmentation dominated	1.0E+07
			Secondary nucleation dominated	1.0E+07
Secondary pathway rate constant	k_-	s^{-1}	Fragmentation dominated	3.1E-07
	k_2	s^{-1}	Secondary nucleation dominated	3.2E-07
Secondary nucleation order	n_2	Unitless	Secondary nucleation dominated	~0
Primary nucleation rate constant	k_n	s^{-1}	Fragmentation dominated	1.1E-08
		s^{-1}	Secondary nucleation dominated	1.1E-08
Primary nucleation order	n_c	Unitless	Fragmentation dominated	~1
			Secondary nucleation dominated	~1

Table S4. Model verification over biological replicates in unseeded assays (N = 3).

Model chosen	Parameter	Symbol	Unit	Average value	Standard deviation
Secondary nucleation dominated, no seed	Combined rate constants	k_+k_n	$M^{-1}s^{-2}$	0.1	0.1
		k_+k_2	$M^{-1}s^{-2}$	22.3	20.1
	Primary nucleation reaction order	n_c	Unitless	~1	0.1
	Secondary nucleation reaction order	n_2	Unitless	~0	0.1
Fragmentation dominated, no seed	Combined rate constants	k_+k_n	$M^{-1}s^{-2}$	7.3	6.6
		k_+k_-	$M^{-1}s^{-2}$	1.7	0.5
	Primary nucleation reaction order	n_c	Unitless	1.4	0.1

Supplementary References

1. Meisl G, Kirkegaard JB, Arosio P, Michaels TC, Vendruscolo M, Dobson CM, Linse S, Knowles TP: **Molecular mechanisms of protein aggregation from global fitting of kinetic models.** *Nat Protoc* 2016, **11:**252-272.